Published in final edited form as:
Conf Proc IEEE Eng Med Biol Soc. 2009 ; 1: 4095. doi:10.1109/IEMBS.2009.5334550.

Off-resonance Saturation Magnetic Resonance Imaging of Superparamagnetic Polymeric Micelles

Chalermchai Khemtong,
Harold C. Simmons Comprehensive Cancer Center, University of Texas Southwestern Medical Center, Dallas, TX 75390-8807 USA

Chase W. Kessinger,
Harold C. Simmons Comprehensive Cancer Center, University of Texas Southwestern Medical Center, Dallas, TX 75390-8807 USA

Osamu Togao,
Advanced Imaging Research Center, University of Texas Southwestern Medical Center, Dallas, TX 75390 USA

Jimin Ren,
Advanced Imaging Research Center, University of Texas Southwestern Medical Center, Dallas, TX 75390 USA

Masaya Takahashi,
Advanced Imaging Research Center, University of Texas Southwestern Medical Center, Dallas, TX 75390 USA

A. Dean Sherry, and
Advanced Imaging Research Center, University of Texas Southwestern Medical Center, Dallas, TX 75390 USA

Jinming Gao
Harold C. Simmons Comprehensive Cancer Center, University of Texas Southwestern Medical Center, Dallas, TX 75390-8807 USA, 214-645-6370; fax: 214-645-6347; jinming.gao@utsouthwestern.edu

Abstract

An off-resonance saturation (ORS) method was used for magnetic resonance imaging of superparamagnetic polymeric micelles (SPPM). SPPM was produced by encapsulating a cluster of magnetite nanoparticles (9.9±0.4 nm in diameter) in poly(ethylene glycol)-b-poly(D,L-lactide) (PEG-PLA) copolymer micelles (micelle diameter: 60±9 nm). In ORS MRI, a selective radiofrequency (RF) pulse was applied at an off-resonance position (0-50 ppm) from the bulk water signal, and the SPPM particles were visualized by the contrast on a division image constructed from two images acquired with and without pre-saturation. Here, the effects of saturation offset frequencies, saturation durations, and RF powers on ORS contrasts were investigated as these parameters are critical for optimization of ORS MRI for *in vivo* imaging applications. The ability to turn “ON” and “OFF” ORS contrast of SPPM solutions permits for an accurate image subtraction and a contrast enhancement to visualize SPPM probes for *in vivo* imaging of cancer.

I. Introduction

Recent development of novel MR probes and new imaging methods with improved imaging sensitivity have rapidly advanced the use of MRI for molecular and cellular imaging of cancer. Compared to the low molecular weight, paramagnetic metal chelates such as Gd-DTPA,

superparamagnetic nanoparticles (e.g., Fe_3O_4 [1,2], $Mn/CoFe_2O_4$ [3], FeCo nanocrystals [4]) have demonstrated substantially higher molar relaxivities and improved sensitivity for *in vivo* MR imaging applications. Once bound to a targeted molecule or after internalization into a cell, superparamagnetic iron oxide (SPIO) probes can create substantial disturbances in the local magnetic field leading to a rapid dephasing of protons and loss of MR signal intensity. Conventionally, T_2- or T_2*-weighted (T_2/T_2*-*w*) MR imaging method was used to visualize SPIO probes where identification of SPIO requires a pre-contrast scan for image subtraction from a post-contrast scan. Very frequently, change of animal position from different MR scans can considerably deteriorate the accuracy of SPIO contrast in subtracted images, leading to poor prognosis of cancer detection. In addition, high concentration of SPIO probes can cause image void on T_2/T_2*-w images, which may be difficult to differentiate from a tissue void (e.g., air sacs in the lung or abdominal cavity) or void-like signals caused by severe magnetic anisotropy that can occur at tissue interfaces.

In this report, we describe the use of superparamagnetic polymeric micelles (SPPM) in combination with an off-resonance saturation (ORS) method as an ultrasenstitive imaging tool for MRI applications. Polymeric micelles are self-assembled nanoparticles from amphiphilic block copolymers, which produce a unique core-shell architecture wherein the hydrophobic core serves as a natural carrier environment for hydrophobic agents and the hydrophilic shell allows particle stabilization in aqueous solution [5,6]. Here we will apply a recently established off-resonance saturation (ORS) method [7,8] to selectively image SPPM contrast. The ORS method involves applying a frequency-selective pre-saturation pulse at an off-resonance frequency from bulk water signal, with the SPPM particles being visualized by the contrast difference between images acquired with ("ON") and without ("OFF") the pre-saturation pulse (Fig. 1a).

II. Materials and Methods

A. Fabrication of SPPM

SPIO nanoparticles (diameter 9.9±0.4 nm, 1 mg in 0.5 mL THF) were mixed well with PEG2k-PLA5k (MW = 7 kD, 5 mg in 0.5 mL THF), and added dropwise into MilliQ water (9 mL) with vigorous agitation using a probe sonicator (60 Sonic Dismembrator, Fisher Scientific). The suspension was left on an orbital shaker overnight to allow THF to evaporate. The SPPM suspension was then filtered through a 1 μm to remove unincorporated SPIO. The solution was subsequently concentrated by a centrifugal filter (MW cutoff 100 kD, MILLIPORE). For iron content ([Fe], μM) in the SPPM solution, an aliquot of the SPPM solution was digested in a concentrated HCl solution before being analyzed by AAS (Varian SpectrAA 50) using a calibration curve based on a Fe standard (Aldrich). Size distribution of the particles was analyzed by TEM.

B. Preparation of the SPPM phantom

Capillary tubes were filled with SPPM solutions of different iron concentrations ([Fe] = 50, 100, 250, 500 μM) and sealed with Parafilm. The capillary tubes were then positioned inside a 5-mL syringe. The syringe was then filled with MilliQ water and sealed using Parafilm.

C. Off-Resonance Saturation MRI of SPPM

All MRI experiments were conducted on a 7 T Varian Scanner (Varian, Palo Alto, CA) at room temperature. The ORS experiment was carried out using a spin-echo pulse sequence modified by the addition of frequency-selective Gaussian-shaped pre-saturation pulse. The phantom study was RF-irradiated at saturation B_1 power of 2.5 and 5 μT at frequency offsets of ±15, 3, 1.5, 1.2, 0.9, 0.6, or 0.3 kHz from the bulk water peak. Reference images were collected using identical settings but without the pre-saturation pulse. The durations of RF-irradiation were

either 200 or 500 ms. Other imaging parameters are as follows: TR = 2 s, TE = 14 ms, FOV = 25×25 mm, slice thickness = 2 mm, matrix = 128 × 128.

D. Data processing

The MRI images were processed using ImageJ (free NIH software: http://rsb.info.nih.gov/ij/). The Mz/Mz^0 division images were generated by pixel-by-pixel division of the saturation-on image by the reference image without pre-saturation. The ORS images were scaled to the same level and no background correction was applied in data processing. The z-spectra of each SPPM solution was obtained by plotting Mz/Mz^0 values versus offset frequencies in ppm.

III. Results

Monodisperse SPIO nanoparticles (Fe_3O_4, 9.9±0.4 nm in diameter) were first synthesized from iron(III) acetylacetonate in benzyl ether according to a published procedure [9]. The SPIO nanoparticles were then encapsulated into PEG-PLA micelles [10]. TEM analysis revealed that the SPPM was monodisperse with an average diameter of 60±9 nm. The schematic illustration and a TEM image of SPPM are shown in Fig. 1b-c. Fig. 1c showed clusters of multiple hydrophobic SPIO nanoparticles inside a hydrophobic depot of the SPPM.

Spin echo MR images (Fig. 2a, top row) showed that off-resonance RF irradiation at 2 ppm from the bulk water darkened the images of the SPPM-containing samples, but not the SPPM-free water. To better illustrate the ORS contrast, we obtained the Mz/Mz^0 division images for all the SPPM samples (Fig. 2a, bottom row). To quantitatively investigate the ORS contrast, we plotted the z-spectra (Mz/Mz^0) as a function of off-resonance frequency in ppm from the bulk water peak at different ORS acquisition conditions (Fig. 2b-e). Data show several trends: first, at the on-resonance saturation frequency (i.e. RF pulse is at the chemical shift of bulk water), the MR signal intensity is dramatically decreased for all the samples including SPPM-free water as expected; second, when the off-resonance frequency is increased, the signal intensity of bulk water quickly returns to normal value (i.e. without RF saturation). In comparison, the SPPM-containing samples demonstrate Fe-induced ORS contrast as illustrated in Fig. 1a; third, under the same ORS acquisition condition, ORS contrast mostly increases with the increase of iron concentrations in the SPPM solutions; lastly, higher B_1 power and longer saturation duration lead to higher ORS contrast. It should be noted that at high B_1 power (e.g. 5 μT) and long duration (e.g. 500 ms), elevated ORS background noise was observed in the SPPM-free water (Fig. 2a), which may reduce the contrast over noise ratios for SPPM detection. Moreover, B_1 power and duration need to be controlled within the safety limit of specific absorption rate (SAR) to minimize radiation exposure in patients.

IV. Conclusions

In summary, we have demonstrated that the ORS technique is a useful tool to enhance contrast effects of SPPM MR probes. A SPPM contrast enhancement by ORS is dependent upon the pre-saturation RF power, pulse duration and frequency offset of the saturation pulse as well as the concentration of SPPM. The quantitative correlation between ORS contrast (Mz/Mz^0) and imaging parameters (e.g. off-resonance frequency, B_1 power and duration) provide the experimental basis to allow for the optimization of acquisition conditions for SPPM detection in biological systems. The combination of ORS imaging with ultrasensitive SPPM design offers new opportunities in tumor-targeted MR imaging for early detection of cancer.

Acknowledgments

This work was supported in part by the National Institute of Health (NIH) under Grants EB005394 and CA129011 (J. Gao), CA15531 and CA126608 (A.D. Sherry), the Robert A. Welch Foundation AT-584 (A.D. Sherry), and the Department of Defense (DOD) BCRP Multidisciplinary Postdoctoral Award W81XWH-06-1-0751 (C. Khemtong).

References

1. Bulte JWM, Kraitchman DL. Iron oxide MR contrast agents for molecular and cellular imaging. NMR Biomed 2004;17(7):484–499. [PubMed: 15526347]
2. Thorek DLJ, Chen A, Czupryna J, Tsourkas A. Superparamagnetic iron oxide nanoparticle probes for molecular imaging. Ann Biomed Eng 2006;34(1):23–38. [PubMed: 16496086]
3. Lee JH, Huh YM, Jun Y, Seo J, Jang J, Song HT, Kim S, Cho EJ, Yoon HG, Suh JS, Cheon J. Artificially engineered magnetic nanoparticles for ultra-sensitive molecular imaging. Nat Med 2007;13(1):95–99. [PubMed: 17187073]
4. Seo WS, Lee JH, Sun X, Suzuki Y, Mann D, Liu Z, Terashima M, Yang PC, McConnell MV, Nishimura DG, Dai H. FeCo/graphitic-shell nanocrystals as advanced magnetic-resonance-imaging and near-infrared agents. Nat Mater 2006;5(12):971–976. [PubMed: 17115025]
5. Sutton D, Nasongkla N, Blanco E, Gao J. Functionalized micellar systems for cancer targeted drug delivery. Pharm Res 2007;24(6):1029–1046. [PubMed: 17385025]
6. Torchilin VP. Multifunctional nanocarriers. Adv Drug Deliver Rev 2006;58(14):1532–1555.
7. Khemtong C, Kessinger CW, Ren JM, Bey EA, Yang SG, Guthi JS, Boothman DA, Sherry AD, Gao JM. In vivo Off-Resonance Saturation Magnetic Resonance Imaging of $\alpha_v\beta_3$-Targeted Superparamagnetic Nanoparticies. Cancer Res 2009;69(4):1651–1658. [PubMed: 19190328]
8. Zurkiya O, Hu X. Off-resonance saturation as a means of generating contrast with superparamagnetic nanoparticles. Magnetic Resonance in Medicine 2006;56(4):726–732. [PubMed: 16941618]
9. Sun SH, Zeng H, Robinson DB, Raoux S, Rice PM, Wang SX, Li GX. Monodisperse MFe_2O_4 (M = Fe, Co, Mn) nanoparticles. Journal of the American Chemical Society 2004;126(1):273–279. [PubMed: 14709092]
10. Ai H, Flask C, Weinberg B, Shuai X, Pagel MD, Farrell D, Duerk J, Gao J. Magnetite-loaded polymeric micelles as ultrasensitive magnetic-resonance probes. Adv Mater 2005;17(16):1949–1952.

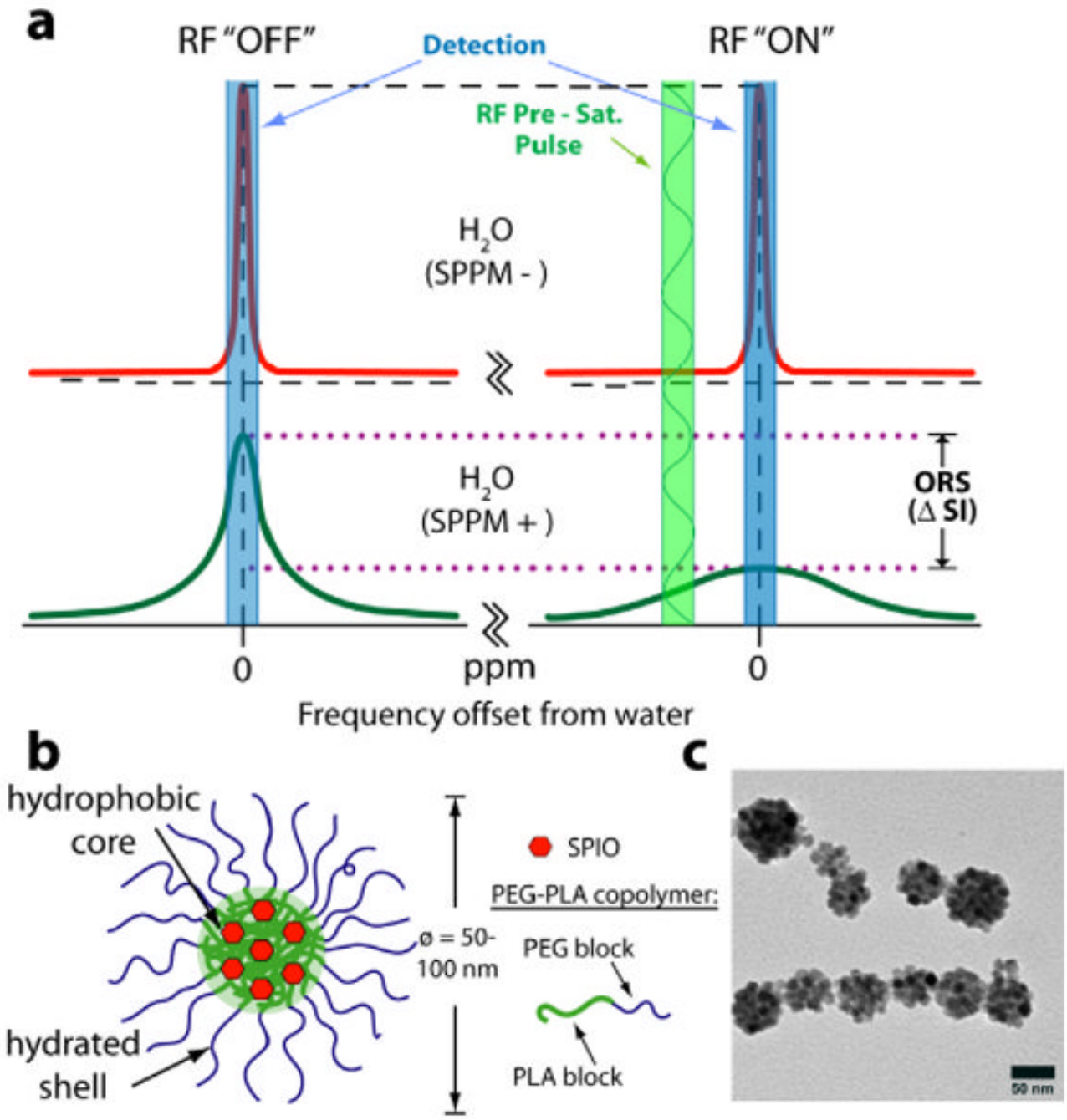

Fig. 1.

(a) Mechanism of SPPM-induced ORS contrast. (b) Schematic illustration of a SPPM particle. (c) TEM image of a representative SPPM sample.

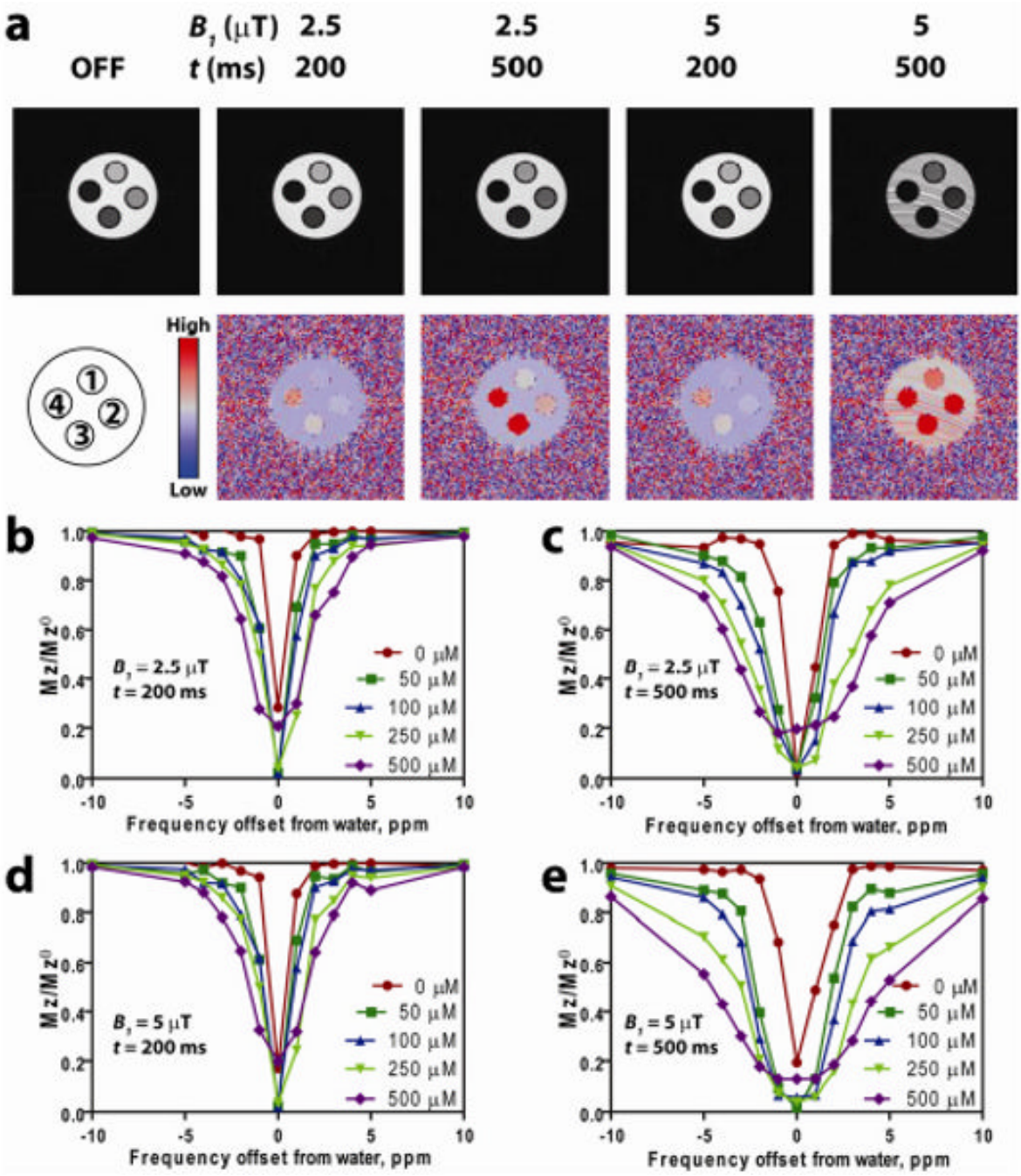

Fig. 2.

(a) Images collected using the indicated pre-saturation pulse power and duration (*top*), and their corresponding ORS images obtained by taking a division of an OFF image with an ON image RF-irradiated at 2 ppm offset. (b-e) *Z*-spectra of SPPM phantoms at different saturation powers and durations. (b) 2.5 μT, 200 ms, (c) 2.5 μT, 500 ms, (d) 5 μT, 200 ms, and (e) 5 μT, 500 ms. Iron concentration in SPPM phantoms are as follows: 1 = 50 μM, 2 = 100 μM, 3 = 250 μM, 4 = 500 μM. The SPPM phantoms are surrounded by water.